ELSEVIER

PII: S0309-1708(98)00006-2

Advances in Water Resources Vol. 22, No. 2, pp. 133–143, 1998

0309-1708/98/$ - see front matter

A non-oscillatory scheme for open channel flows

Scott A. Yost & Prasad M. S. V. Rao

161 CE/KTC Bldg., Department of Civil Engineering, The University of Kentucky, Lexington, KY 40506-0281, USA

(Received 3 September 1997; revised 6 January 1998; accepted 2 March 1998)

In modeling shocks in open channel flows, the traditional finite difference schemes become inefficient and warrant special numerical treatment for smooth computations. This paper provides a general introduction to the non-oscillatory high-resolution methodology, coupled with the advantages of using these conservative methods for open channel applications. Results of the numerical experiments are presented and compared to standard algorithm results, analytical solutions and experimental results to demonstrate the robustness of the high-resolution formulation. Finally results of flows with mixed flow conditions (as in hydraulic jump), indicate that the contribution of the Boussinesq pressure term is minimal. Besides showing robustness in capturing shocks in open channel, the results indicate that the effect of the grid spacing on the shock resolution is small. However, for jumps with high Froude numbers, the present formulation slightly underestimates the peak depth. © 1998 Elsevier Science Limited. All rights reserved

Keywords: high resolution, flux splitting, non-oscillatory, surge, hydraulic jump.

1 INTRODUCTION

A major difficulty in the numerical approximation of nonlinear hyperbolic conservation laws is the presence of discontinuities in the solution. Traditional Finite Difference schemes (i.e., Lax–Wendroff, MacCormack) generate spurious oscillations in the numerical solution in the vicinity of the discontinuities. A characteristic feature of all central Finite Difference (FD) schemes of 2^{nd}-order or greater accuracy is that they produce dispersive errors in capturing the shock profile. Suppressing these oscillations in the vicinity of the shock requires the addition of artificial smoothing terms. The FD schemes also have a poor shock-capturing ability in terms of their resolution. The shock discontinuity often transverses several grid nodes. In reality, discontinuities in the physical flow field, referred to as shock waves, do not exhibit oscillations. On the other hand, the corresponding numerical solution with higher-order accurate (≥ 2) schemes exhibits oscillations. These oscillations are purely of numerical origin. To overcome the above two limitations, standard methods based on central differencing, together with artificial viscosity, have often been replaced by high-resolution shock-capturing schemes.

To enjoy the advantages of higher-order schemes, coupled with an oscillatory free solution, over the past decade the focus has shifted toward developing and solving the flow equations with high-resolution schemes. These include the Total Variation Diminishing (TVD) schemes of Harten,[12] Flux Corrected Transport (FCT) methods of Boris and Brook[5] and Zalesak,[25] switches and cell-averaged piecewise fits utilized in the Piecewise Parabolic Method (PPM) of Collela and Woodward[7] and the Essentially Non-oscillatory (ENO) schemes of Harten and Osher.[13] The basic idea in all theses high-resolution schemes can be traced back to the work of Vanleer.[23]

A distinct difference exists between high-resolution schemes and higher-order central finite differencing schemes, which needs explanation. Central difference schemes, which do not have high-resolution shock-capturing ability, always result in oscillations (non-monotonous solution). The addition of artificial viscosity simply suppresses these oscillations but does not totally eliminate them. In this sense, the artificial viscosity can be thought of as a 'filtering mechanism', which filters the oscillations after they are produced by the basic numerical solution. To make the present discussion self complete, we briefly touch upon the results of Berger and Stockstill,[4] who had applied a Streamline Upwind Petrov–Galerkin (SUPG) formulation for open channel flows. They had smoothed the oscillations by changing the magnitude of upwinding parameter (a

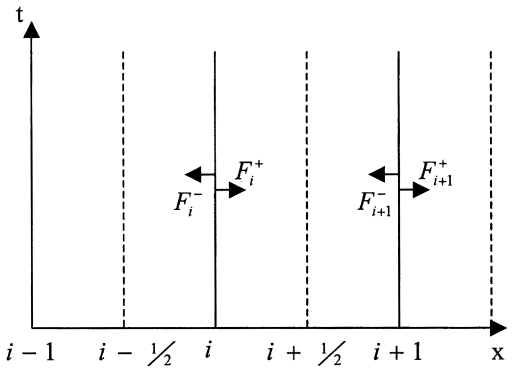

Fig. 1. Sketch of positive and negative flux contribution at any grid node.

dimensionless number), whose value depends on the degree of oscillations present in the computational domain. Correlating their formulation to the standard Finite-difference algorithms, the oscillations are allowed to form and then smoothed by keeping a track of the shock-front. In contrast to this role of artificial viscosity (or filtering), when a high-resolution scheme is used, numerically induced oscillations are *prevented* from occurring (a feature that is incorporated in the basic flux differencing methodology), not just filtered away.

As the ENO formulations have proven to have an edge over the other high-resolution formulations cited above in other applications, its performance in solving the one-dimensional open channel flow equations is investigated. The family of ENO schemes constructed in Harten and Osher[13] use both cell averages and point values of the flow variables in the discretization of the spatial flux terms. Reconstructing the flow variables at the grid nodes, before the solution is marched to the next time level is often complicated. Shu and Osher,[22] after detailing this problem, simplified the implementation of the ENO schemes by using a Lax–Friedrich (LF) type of discretization for the spatial flux terms. The formulation presented in the next section is very similar to their findings. The ENO methods (also referred to as Non-Oscillatory methods) are an improvement over the TVD schemes, generate oscillatory free solutions and have high-resolution shock-capturing ability as a built-in feature. Methods based on the ENO formulation manifest many properties desirable in numerical simulations. The conservation property, the avoidance of numerical oscillations, the adherence to signal propagation principles, and the achievement of higher order accuracy makes the ENO schemes a robust tool in solving the open channel flow problems.

The objective of this work is to illustrate that a high-resolution shock-capturing scheme is more robust, efficient and simpler both in formulation and programming for simulating open channel flows. Emphasis here is laid more on the numerical results, while rigorous analytical and theoretical proofs can be found in the references cited.

2 GOVERNING EQUATION AND THE NUMERICAL FORMULATION

The high-resolution ENO method is applied to the equations that govern open channel flow. The basic governing flow equations for one-dimensional flows can be written as[6]

$$[U]_t + [F]_x = [S] \tag{1}$$

where the elements of

$$[U] = \begin{bmatrix} h \\ q \end{bmatrix}, [F] = \begin{bmatrix} q \\ \dfrac{q^2}{h} + \dfrac{gh^2}{2} \end{bmatrix}, \text{and } [S] = \begin{bmatrix} 0 \\ gh(S_o - S_f) \end{bmatrix}$$

in which h is the flow depth, q is the specific discharge, g is the gravity term, S_o is the bottom slope of the channel and S_f is the friction slope, which is computed from Manning's equation. Starting from the initial time level, n, where the values of the flow variables are known, the solution, based on the explicit finite difference discretization, at the unknown time level, $n+1$, is obtained as

$$U_i^{n+1} = U_i^n - \frac{\Delta t}{\Delta x}\left(\hat{F}_{i+\frac{1}{2}} - \hat{F}_{i-\frac{1}{2}}\right) + \Delta t[S] \tag{2}$$

In eqn (2), Δt is the time step, which is computed using the Courant-Friedrich-Lewis (CFL) stability condition,

$$\Delta t = C_n \frac{\Delta x}{\max(u + \sqrt{gh})}$$

Δx is the spatial grid increment, u is the flow velocity, C_n (≤ 1) is the Courant number (0.9 in the present work) and $\hat{F}_{i\pm 1/2}$ are the split fluxes at the cell interfaces.

With reference to Fig. 1, the flux contribution at any grid node is decomposed to its positive and negative components whose magnitude is given as

$$F_i^+ = 0.5(F_i + \alpha U_i) \tag{3}$$

$$F_i^- = 0.5(F_i - \alpha U_i) \tag{4}$$

where $\alpha \geq \max(\lambda_{1,2})$ in which λ is the two eigen values of the Jacobian matrix, $\partial F/\partial U$. For the system of equations represented by eqn (1), the eigen values are $\lambda_{1,2} = (u \pm \sqrt{gh})$. Conversely, eqns (3) and (4) imply that the total flux at any grid node is the summation of its positive and negative components, or

$$F_i = F_i^+ + F_i^- \tag{5}$$

At the cell interfaces, $i \pm \dfrac{1}{2}$, the spatial flux terms are computed as

$$\hat{F}_{i+\frac{1}{2}} = \hat{F}^+_{i+\frac{1}{2}} + \hat{F}^-_{i+\frac{1}{2}} \tag{6}$$

$$\hat{F}^+_{i+\frac{1}{2}} = F_i^+ + 0.5\Delta F_i^+ \tag{7}$$

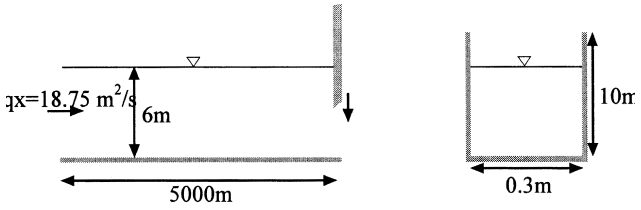

Fig. 2. Definition sketch for sudden closing of a gate.[9]

$$\hat{F}^{-}_{i+\frac{1}{2}} = F^{-}_{i+1} - 0.5\Delta F^{-}_{i+1} \tag{8}$$

The function ΔF is the flux limiter and is responsible for obtaining monotonous (oscillation free) solutions.

Comparing eqn (2) to any other finite difference discretization method (Lax–Wendroff, MacCormack) reveals the basic difference between the central differencing and the high-resolution schemes. While in the former, the fluxes, F, at the grid nodes directly contribute to the spatial discretization, the latter differ by using the split fluxes, $\hat{F}$. Evaluation of the split fluxes, eqn (6) takes into account both the direction of propagation of wave ($F^{\pm}$, eqns (3)–(5)) and the restricted flux gradients through the use of limiters ($\Delta F^{\pm}$, eqns (9) and (10)) to ensure an oscillatory free solution, aspect absent in the central differencing formulation.

In the present work, the limiter was computed using the *minmod* function (Hirsch[15]). This flux limiter can be expressed as

$$\Delta F_i^{+} = \text{minmod}\left(F^{+}_{i+1} - F_i^{+}, F_i^{+} - F^{+}_{i-1}\right) \tag{9}$$

$$\Delta F_i^{-} = \text{minmod}\left(F_i^{-} - F^{-}_{i-1}, F^{-}_{i+1} - F_i^{-}\right) \tag{10}$$

The *minmod* function between two variables is defined as

$$minmod(a,b) = \begin{cases} a \text{ if } |a| < |b| \text{ and } ab \geq 0 \\ b \text{ if } |b| < |a| \text{ and } ab \geq 0 \\ 0 \text{ if } ab < 0 \end{cases} \tag{11}$$

Eqn (11) indicates that the *minmod* operator, and hence the flux limiter, can take three values. When the two arguments a and b are of opposite sign, the value returned by the operator is zero. When the two arguments are of the same sign, the operator chooses a or b depending on which has a smaller value. In addition to this limiter, the other limiters that have found wide application are *cmplim* (compressive flux limiter), Vanleer's limiter and Roe's *superbee* limiter.[15]

3 APPLICATIONS

With the highlights of the numerical scheme outlined, extensive tests have been performed to study the method's performance on a wide variety of one-dimensional open channel flows, with particular focus on its shock-capturing ability. To illustrate the method, results are presented for shocks formed by surges (i.e., sudden opening and closing of a gate), oscillating wave, dam break on wet bed and formation of a hydraulic jump. The first three examples have been selected for benchmarking purposes. As analytical solutions are available these tests demonstrate the advantages built into the present technique and illustrate the ENO's robustness compared to current state-of-the-art techniques reported in the literature. Lastly results of a hydraulic jump for different Froude numbers are compared to experimental and other computational results. For all the cases studied here, a Courant number of 0.9 is used in determining the time step based on the CFL stability condition.

3.1 Simulation of surges

Surges in open channels frequently arise due to either a sudden opening or closing of a control gate. The hydraulic events that follow sudden gate movement are important aspects in the design of channels. The resulting flow, which is unsteady and rapidly varying, commonly occurs in sudden release of discharge from a power plant or from a reservoir. In particular, satisfactory prediction of both the arrival of wave front and its depth are sought. As analytical solutions are available for horizontal smooth channels, they can also be used as a benchmark for comparison to the shock-capturing ability of a numerical scheme.

3.1.1 Sudden closure of a gate

The hydraulic characteristics arising out of a sudden closure of downstream gate are presented in this section. For comparison purposes, the present numerical scheme is applied to problems with data reported in the literature.[9] The definition sketch of the problem is shown in Fig. 2. The test problem consists of a horizontal smooth rectangular channel 5000 m long with an initial depth and specific discharge of 6 m and 18.75 m^2/s, respectively. A surge was created at the downstream end by an instantaneous closure of the gate. For the computations, initial conditions of $h = 6$ m and $q_x = 18.75$ m^2/s were specified throughout the channel domain. Numerically, specifying a zero discharge at the downstream end for all time levels creates the surge wave. Physically this corresponds to the case of an instantaneous closure of the gate. The other flow variable at the downstream boundary (i.e., flow depth) was calculated using the C^+ characteristic curve resulting from eqn (1) (Chaudhry[6]). As the wave front does not reach the upstream boundary for the time period simulated, no specific boundary condition was specified upstream. Thus the flow variables were kept equal to the initial values. The analytical solution for the above problem derived by Abbott[1] is used as the benchmark.

The gate closure was simulated with a grid spacing of 10 m until the wave reached the upstream boundary. Fig. 3 compares the transient profiles to the analytical solution at two different times, $141 + \Delta t$ s and $354 + \Delta t$ s. The plot indicates that the present ENO formulation can capture the shock front with no significant dissipation or spurious oscillations. Furthermore, the shock is captured in one Δx, the best possible outcome, indicating the high resolution of the shock front. Fig. 4 plots the cumulative variation of

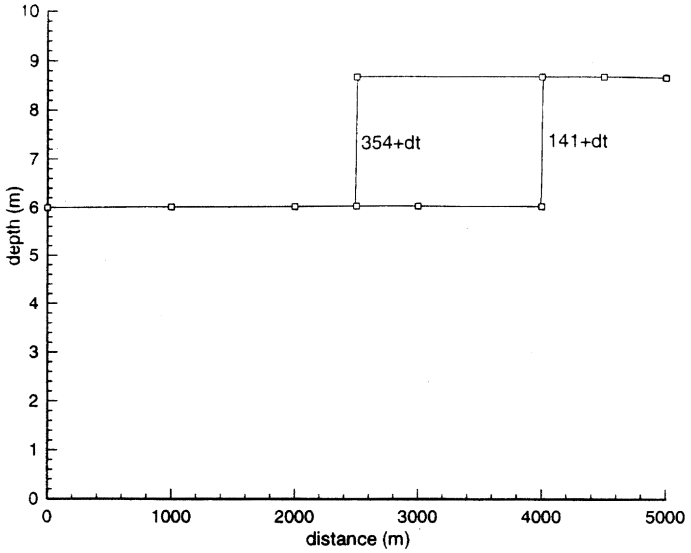

Fig. 3. Transient profiles for sudden closing of a gate (— computed, □ analytical solution[1]).

the error

$$\sqrt{\sum_{\text{gridnodes}} \left(h_{\text{exact}} - h_{\text{cal}}\right)^2}$$

as a function of the number of grid nodes, when the shock is at mid-section ($t \approx 354$ s). This plot shows the close agreement between the analytical and numerical solutions, almost independent of grid resolution.

3.1.2 Sudden opening of a gate

A sudden opening of the gate is simulated by a sudden increase in the discharge at the upstream end of the channel containing a uniform water depth and no flow. The definition sketch of the problem is illustrated in Fig. 5. The initial condition in the 2000 m long frictionless channel is a uniform depth of 1 m with $q_x = 0\ \text{m}^2/\text{s}$. At the upstream boundary, a discharge of $10\ \text{m}^2/\text{s}$ is specified at time $t = 0^+$. The flow depth at the upstream boundary is computed from the C^- characteristic. At the downstream end, no boundary conditions are specified and the flow variables are kept at their initial values.

The gate opening was simulated with a grid spacing of $\Delta x = 4$ m until the wave reached the downstream boundary. The captured shock front at two time levels ($100 + \Delta t$ s and $200 + \Delta t$ s) is plotted in Fig. 6 along with the analytical solution. The predicted values of the celerity and the height of the wave front are in close agreement with the analytical solution with no visible oscillations evident near the shock front.

3.2 Modeling an oscillatory wave

This numerical test is concerned with the modeling of free oscillation in a horizontal frictionless rectangular channel that has an open boundary at the inlet and a closed boundary at the outlet. When it was first introduced into the field of computational hydraulics, Garcia and Kahawita[10] first performed this test, which is considered to be an extreme challenge for numerical models,[19] using the MacCormack scheme. Numerically, this test is accomplished by specifying an initial depth ($h_0 = 10$ m) and zero velocity ($q_x = 0\ \text{m}^2/\text{s}$) throughout the channel. Then a disturbance is created at the upstream boundary by suddenly increasing the depth ($h_t = 10.1$ m at $t = 0^+$), which is then held constant for all times. At the downstream end, a zero discharge is specified for all time, replicating a closed boundary. The other flow variables at the upstream and downstream boundary are computed from the C^- and C^+ characteristic curves, respectively.

These specified boundary conditions generate a traveling wave whose wave height is constantly changing h_0 between $\pm$ 0.2 as it reflects at the downstream boundary. The ability of the ENO scheme to capture this oscillatory wave nature is

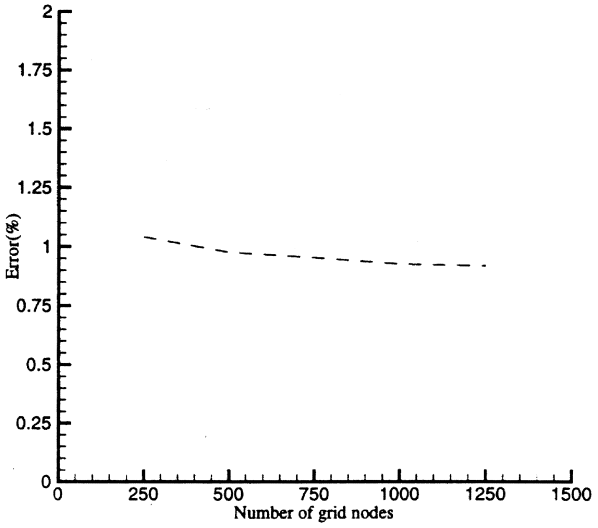

Fig. 4. Error distribution for various grid sizes.

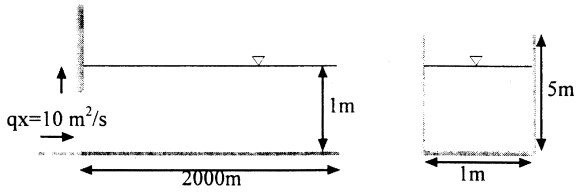

Fig. 5. Definition sketch for sudden opening of a gate.

presented in Fig. 7, which shows the time evolution of depth at the downstream boundary. A numerical scheme is considered satisfactory if it can reproduce the celerity and the time period accurately. The plot indicates that the computed depth, which is a step function of time with period equal to 2000 s, is in close agreement to the analytical solution. No significant amounts of dissipation or oscillations are observed, even for larger time periods, indicating the reliability of the present algorithm. To further show the robustness of the algorithm, the transient discharge (q) at the upstream boundary is plotted in Fig. 8.

3.3 Dam-break problem

Studying the movement of flood waves resulting from a sudden collapse of a dam has drawn significant attention of many numerical investigators. Depending on the flow conditions downstream, both dry-bed and wet-bed flow conditions have been studied.[3,8,18] Until now, all the numerical models based on differencing techniques have used the central schemes, which includes both explicit and implicit formulations. To facilitate a comparison of the latest results reported in the literature, the present model has been run for the test conditions of Rahman and Chaudhry.[21]

As pointed out earlier, standard finite difference schemes have a poor shock-capturing ability. While the first-order accurate schemes smear the shock front, the second- and higher-order schemes produce dispersive errors in the vicinity of the discontinuity. A satisfactory simulation would involve smoothing these oscillations, which in general means the introduction of some type of artificial viscosity.

In addition to the above limitation of the central schemes, there are other limitations regarding the poor resolution in capturing the shock front (i.e., the shock front often spreads over several grid nodes). Numerical strategies are needed to obtain a high-resolution shock front. To this end, Rahman and Chaudhry[20,21] employed the use of a dynamic grid adaptation technique. Using the explicit MacCormack scheme, they solved the flow equations in conjunction with an extra grid equation in an uncoupled manner. The grid spacing between the nodes near the shock front is decreased in an interactive manner, so as to reduce the possible smearing. The underlying assumption being that a large uniform grid spacing results in the smearing of the shock, and small uniform grid spacing is computationally uneconomical. The spurious oscillations produced by the MacCormack scheme were smoothed using the procedure outlined in Jameson *et al.*[16]

The present ENO formulation contains high-resolution shock-capturing ability as a characteristic feature. No additional numerical mechanism needs to be coupled, to the basic procedure for achieving monotonous results. Specifically, the application of any additional smoothing can be avoided.

For comparison to published results, the test problem illustrated in Fig. 9 is simulated. With the initial depths of $h_0 = 10$ m upstream and $h_0 = 6$ m downstream of the dam specified, the dam is removed at time $t = 0^+$. The transient flow profiles for $t = 60$ s after the release are plotted in Fig. 10. The corresponding plot as obtained by Rahman and Chaudhry[21] is shown in Fig. 11, which includes results from several methods, including their adaptive grid technique. A comparison of Figs 10 and 11 indicates that even though a uniform grid spacing is used in this work, the results are in good agreement with the analytical solution

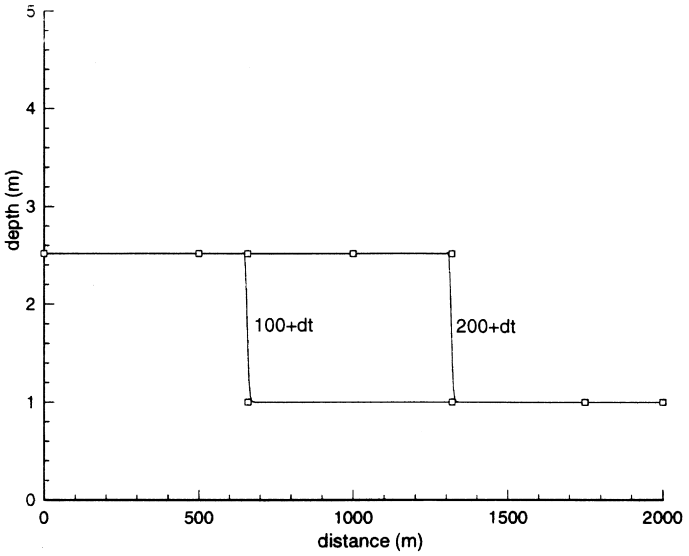

Fig. 6. Transient profiles for sudden opening of a gate (— computed, □ analytical solution).

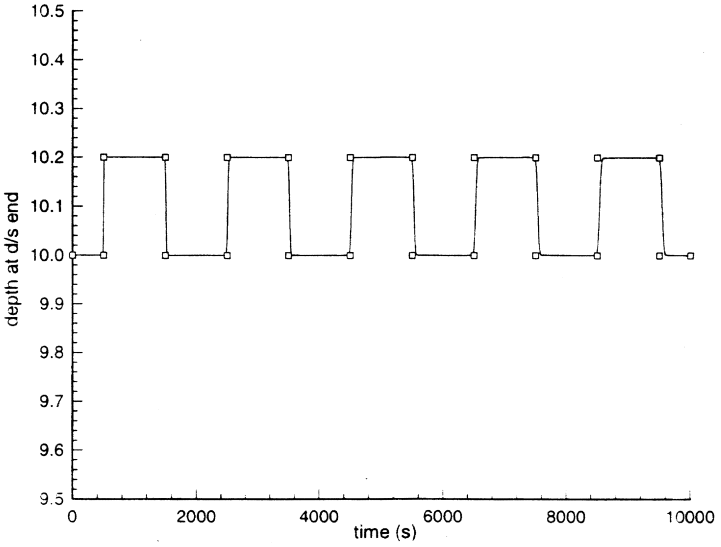

Fig. 7. Profile of oscillatory wave at downstream boundary (— computed, □ analytical solution).

and are similar to the other numerical results. In addition, for comparison to Rahman and Chaudhry, our grid spacing ($\Delta x = 25$ m) is equal to their initial uniform spacing. The point we want to stress is the simplicity of the present formulation. Without introducing artificial viscosity or solving extra grid equations, we are able to obtain reasonable results with state-of-the-art methods. Additional comparisons with the MacCormack scheme coupled with grid adaptation and artificial viscosity, are presented in the next section.

3.4 Simulation of hydraulic jump

The capacity of the model to simulate mixed flow conditions can be best tested in simulating a hydraulic jump, which is a challenging problem because of its complex nature. The hydraulic jump is formed whenever flow transitions from supercritical to subcritical. Given its wide importance in open channel hydraulics, a proper simulation involves a satisfactory prediction of the location and height of the jump.

The present numerical model has been run to represent the experimental data of Gharangik and Chaudhry.[11] As reported, the test flume is 14 m long and 0.46 m wide. By suitably controlling the depth at the downstream end, the jump was allowed to form in the first 3 m of the glassed flume. The Manning's roughness coefficient varied between 0.008 to 0.011, depending on the depth. The experiments were conducted for Froude numbers varying from 2.3 to 7.0. To conserve space and without loss of generality, the results for two Froude numbers are presented. The flow variables for these Froude numbers are summarized in Table 1. Those interested in additional experimental information are referred to the original reference.[11]

Though various techniques have been proposed to improve the shock-capturing ability of the standard methods and tested for different flow cases,[14,17] their capacity to

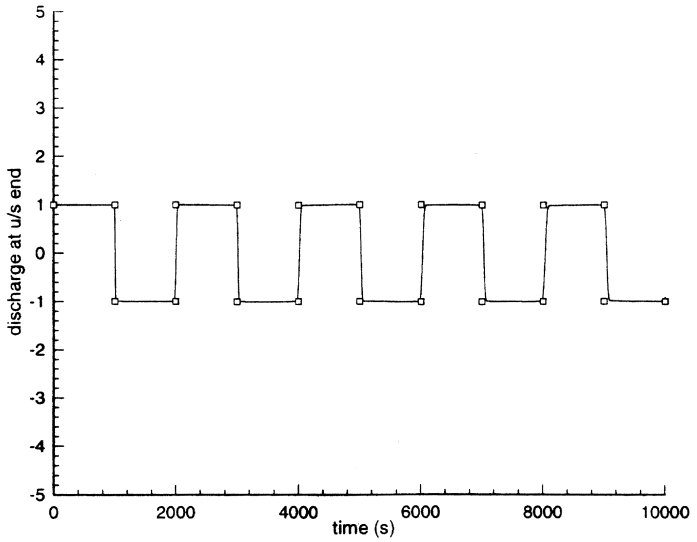

Fig. 8. Transient discharge of oscillatory wave at upstream boundary (— computed, □ analytical solution).

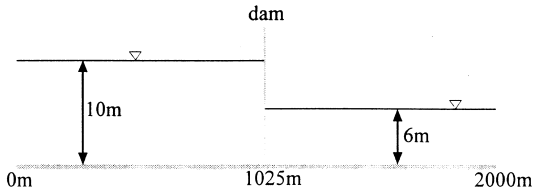

Fig. 9. Definition sketch for dam break problem on a wet bed.

simulate hydraulic jump have not been investigated. Regardless of historical precedence, the hydraulic jump has significant practical importance in hydraulics, not to mention its a challenging problem. On the numerical front, St. Venant equations have been widely used for simulating the phenomenon, with both Finite Difference and Finite Element techniques. The underlying assumption in the derivation of the St. Venant equations is the hydrostatic pressure distribution. As pointed out by Witham[24] and Basco,[2] this assumption may not be valid for rapidly varying flows, a characteristic of the hydraulic jump. To correct this inconsistency, they corrected the pressure term by adding the Boussinesq term, which accounts for the sharp streamline curvature. Gharangik and Chaudhry,[11] Rahman and Chaudhry[20] and Basco[2] have numerically solved the resulting flow equations, often referred to as the one-dimensional Boussinesq equations, by using a FD discretization for the spatial flux terms.

3.4.1 Initial and boundary conditions

In the simulation of the hydraulic jump, initially the flow is assumed to be supercritical throughout the channel. Starting with the specified initial conditions at the upstream end (Table 1), the flow parameters at the other nodes are obtained by integrating the gradually varied flow equation.[6] As the flow is supercritical at the upstream end, it can be shown using the method of characteristics that the boundary conditions for all flow variables must be specified at the upstream boundary. Hence, the flow depth and discharge at upstream boundary are held constant for the entire simulation, equal to the initial values. At the downstream end, a constant flow depth is specified only, again based on the method of characteristics. This specified depth is held constant for all time periods. The other flow variable (discharge) is computed from the C^+ (positive) characteristic of eqn (1) (Chaudhry[6]).

Since the focus is the steady-state solution, a false transient approach was used. In this approach, the steady-state solution is obtained by using time as the iteration parameter. Starting from the initial conditions ($t = 0$), the solution progresses in time until reaching a steady-state convergence. Coupled with the boundary conditions, the numerical approach outlined above can be used for computing the unknowns at all the interior grid nodes.

3.4.2 Results and discussion

It was shown for several traditional test problems involving shocks that the ENO scheme presented here gives reasonable results when compared to analytical solutions and current state-of-the-art numerical procedures. In obtaining these results, this approach overcomes the traditional problems of either diffusing the wave front (1st order methods) or causing spurious oscillations at the shock front (2nd order methods) without using artificial viscosity or grid adaptation. After the method's robustness was shown for simple problems, the more difficult hydraulic jump is investigated.

The ENO method is applied to the two different Froude Number cases. Figs 12 and 13 show the stationary hydraulic jump profiles for Froude numbers of 4.23 and 6.65, respectively, along with the experimental results. The method captures the jump without oscillation at the shock front, independent of the Froude number. It appears the method slightly disperses the jump. However, Figs 14 and 15 show

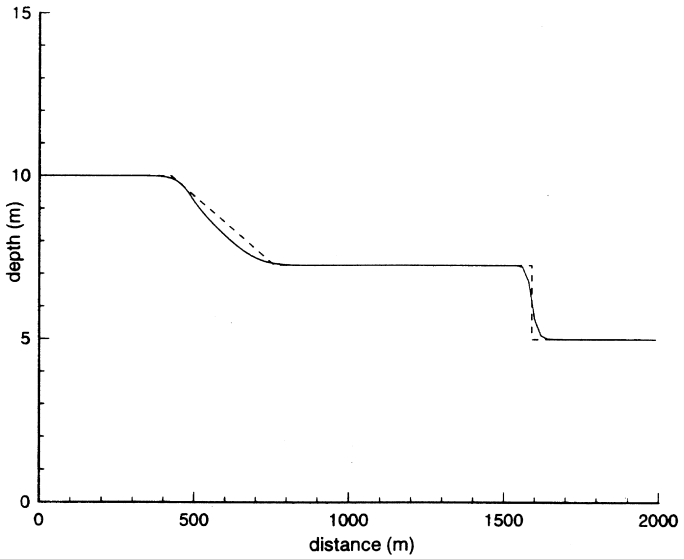

Fig. 10. Transient flow profile for dam break (— computed, - - - analytical solution).

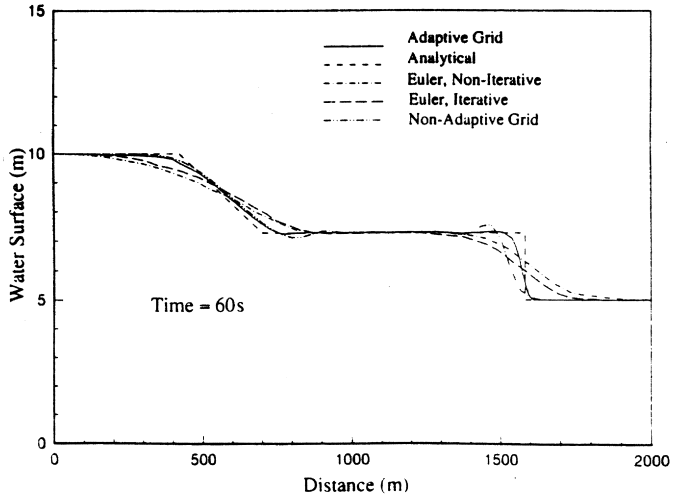

Fig. 11. Transient flow profiles for dam break as reported in Rahman and Chaudhry.[21]

that the crispness of the front is slightly improved by reducing the grid spacing from 0.28 m to 0.14 m. While the resolution of the shock front in the central schemes dramatically improves as the grid spacing is reduced, Figs 14 and 15 indicate that doubling the grid spacing has little effect on the shock resolution of this ENO method. The shock front continues to form primarily between the two adjacent grid nodes. Though the results are not included, the present trends are also evident for simulated flows with other Froude numbers ($F_r = 2.3$, 5.74 and 7.00).

The derivation of eqn (1) involves the assumption of a hydrostatic pressure distribution. For flows with low Froude numbers (weak hydraulic jumps), this assumption is valid, and the solution obtained by using any shock-capturing numerical techniques is satisfactory. However, for flows with high Froude numbers this assumption may not be valid, and hence the Boussinesq equation, which takes into account the non-hydrostatic pressure distribution, is more appropriate. As we make the case for using eqn (1) in the present investigation of hydraulic jumps, others have studied the error associated with the hydrostatic assumption. Both Rahman and Chaudhry[20] and Gharangik and Chaudhry[11] conducted an order-of-magnitude analysis of the Boussinesq pressure term. They concluded that in stationary jumps, its contribution is very small near the jump and negligible at regions away from it. Based on their observations, the MacCormack scheme was used in their computations. However, in order to improve the shock resolving capacity of the MacCormack scheme while smoothing the solution, Rahman and Chaudhry[20] implemented a grid adaptation technique. Their analysis for higher Froude numbers indicates that as long as the scheme has a high-resolution shock-capturing ability, the equations with or without the Boussinesq term yield similar results.

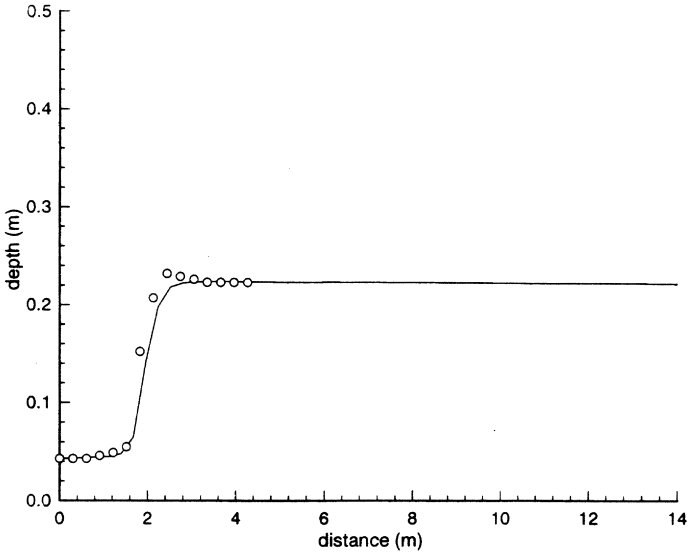

Fig. 12. Hydraulic jump steady state profiles for $F_r = 4.23$ (— computed, ○ experimental[11]).

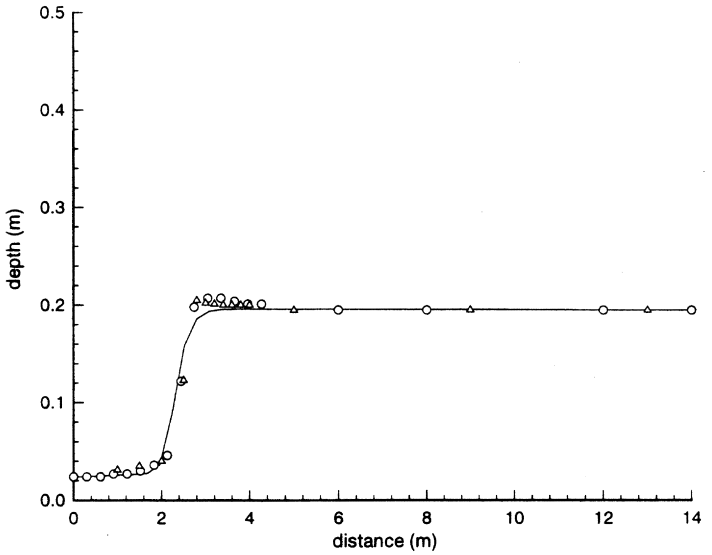

Fig. 13. Hydraulic jump steady state profile for $F_r = 6.65$ (△ computed,[20] — computed, ○ experimental[11]).

High-resolution shock-capturing ability is an inherent feature of the ENO schemes. Thus no extra grid equation needs to be solved for this purpose. Fig. 13 shows that the inclusion of the Boussinesq terms in the governing equations is not needed. The results have also been compared with those of Rahman and Chaudhry,[20] who have included the higher order pressure terms. A comparison with the experimental values indicates that while the location of the shock front is predicted accurately, the maximum depth is slightly underestimated. A possible theoretical explanation for this is that the schemes based on the ENO formulation have a reduced order of accuracy at the extreme points. As pointed out by Shu and Osher,[22] this may result in the reduction of accuracy in small regions on either side of the extreme point.

The evolution of the shock at different time periods is illustrated in Figs 16 and 17 for the two cases ($F_r = 4.23$, $F_r = 6.65$). The plot indicates that the flow profile travels to a distance of 1.5 m from the upstream boundary ($t \approx 50$ s) before being pushed back to its stationary location by the supercritical flow. At no stage of the evolution are oscillations evident. A grid spacing of 0.28 m was used for generating the above plots. Finally, a check on the mass continuity at steady state for the two flow conditions is summarized in Table 2. The small residual error indicates that the present formulation conserves mass in its numerical discretization.

4 CONCLUSIONS

The basic flow equations of one-dimensional open channel flow have been solved using a high-resolution

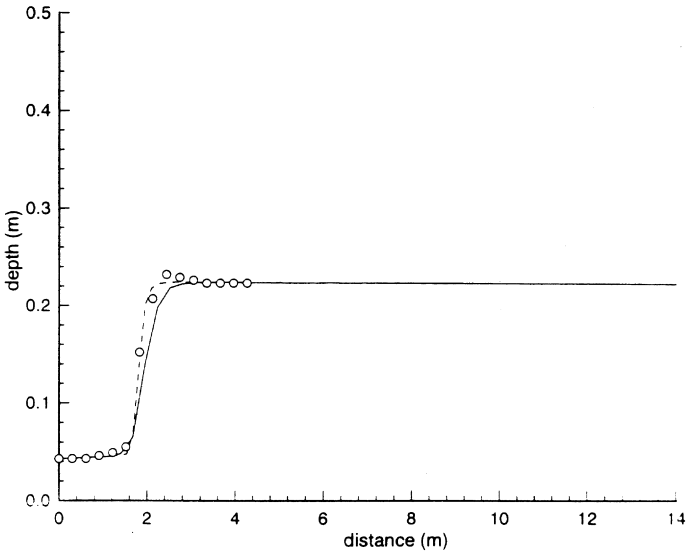

Fig. 14. Effect of grid spacing on shock reduction, $F_r = 4.23$ (— $\Delta x = 0.28$, - - - $\Delta x = 0.14$, ○ experimental[11]).

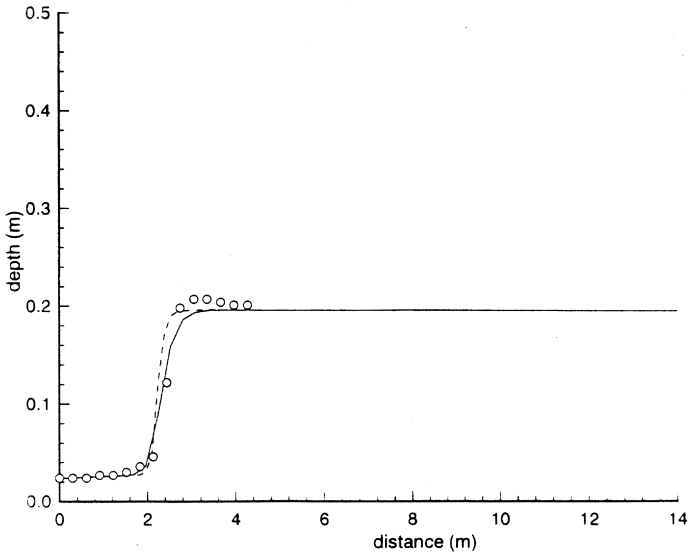

Fig. 15. Effect of grid spacing on shock reduction, $F_r = 6.65$ (— $\Delta x = 0.28$, - - - $\Delta x = 0.14$, ○ experimental[11]).

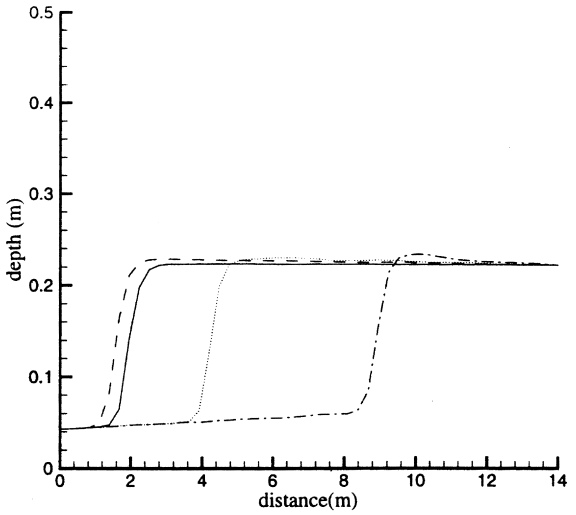

Fig. 16. Shock profile for $F_r = 4.23$: – · – $t = 10.06$ s, · · · $t = 25.06$ s, - - - $t = 50.07$ s, — $t = 100.02$ s (steady-state).

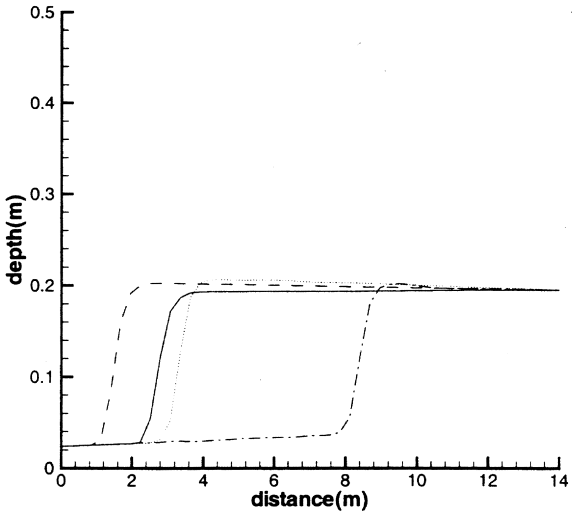

Fig. 17. Shock profile for $F_r = 6.65$: – · – $t = 10.06$ s, · · · $t = 25.05$ s, - - - $t = 50.03$ s, — $t = 75.02$ s (steady-state).

Table 1. Test conditions for hydraulic jump[11]

Test no.	Upstream depth (m)	Upstream velocity (m/s)	Downstream depth (m)	Froude number
1	0.043	2.737	0.222	4.23
2	0.024	3.255	0.195	6.65

Table 2. Mass residual error for various Froude numbers

Froude number	Mass residual error($\times 10^{-4}$)
4.23	5.06
6.65	2.54

shock-capturing scheme. The method's performance was tested on various open channel flow problems. The results indicate that the method is comparable to current state-of-the-art methods that use standard techniques coupled with numerical smoothing techniques. The present scheme has an inherent high-resolution shock-capturing ability so that no special numerical smoothing is needed. Furthermore, as opposed to the Central Finite Difference schemes, the effect of grid spacing on the shock resolution is minimal. Extensive tests have been carried out to justify the robustness of the method. The results obtained while simulating various hydraulic jumps support other's conclusions that the contribution of Boussinesq terms (non-hydrostatic pressure) near the shock is minimum and satisfactory results can be

obtained by solving the St. Venant equations with a robust shock-capturing scheme. A test of the mass residual error at steady state shows that the present formulation is also conservative. Thus it is concluded that the present model, and more generally the high-resolution schemes, can be reliable and robust tools in predicting the location of shock fronts in open channels without added diffusion or spurious oscillations.

ACKNOWLEDGEMENTS

The authors would like to thank Elsevier Science Ltd. for their permission to reproduce Fig. 11, which was originally published in *Advances in Water Resources*, 1998, **21,** 1–9.[21]

REFERENCES

1. Abbott, M. B., *Computational Hydraulics: Elements of Theory of Free Surface Flows*, Pitman, London, 1979.
2. Basco, D. R. Limitations of de Saint Venant equations in dam-break analysis. *J. Hydraul. Eng.*, 1989, **115,** 950–965.
3. Bellos, C. V. and Sakkas, J. G. 1-d dam break flood wave propagation on dry bed. *J. Hydraul. Eng.*, 1987, **113,** 1510–1524.
4. Berger, R. C. and Stockstill, R. L. Finite-element model for high-velocity channels. *J. Hydraul. Eng.*, 1995, **121,** 710–716.
5. Boris, J. P. and Brook, L. D. Flux corrected transport, SHASTA, a fluid transport algorithm that works. *J. Comput. Phys.*, 1973, **11,** 38–69.
6. Chaudhry, M. H., *Open Channel Flows*, Prentice-Hall, Englewood Cliffs, NJ, 1995.
7. Collela, P. and Woodward, P. R. The piecewise parabolic method (PPM) for gas dynamics simulation. *J. Comput. Phys.*, 1984, **54,** 174–201.
8. Dammuller, D. C., Bhallamudi, S. M. and Chaudhry, M. H. Modeling of unsteady flow in curved channel. *J. Hydraul. Eng.*, 1988, **115,** 1479–1495.
9. Fennema, R. J. and Chaudhry, M. H. Explicit numerical schemes for unsteady free surface flows with shocks. *Water Resources Research*, 1986, **22,** 1923–1930.
10. Garcia, R. and Kahawita, R. A. Numerical simulation of St. Venant's equations with the MacCormack finite difference scheme. *Int. J. Num. Methods Fluids*, 1986, **6,** 259–274.
11. Gharangik, A. M. and Chaudhry, M. H. Numerical simulation of Hydraulic jump. *J. Hydraul. Eng.*, 1991, **117,** 1195–1211.
12. Harten, A. High-resolution schemes for Hyperbolic Conservation laws. *J. Comput. Phys.*, 1983, **49,** 357–393.
13. Harten, A. and Osher, S. Uniformly high order accurate non-oscillatory schemes. *SIAM*, 1987, **24,** 279–310.
14. Hicks, F. E., Steffler, P. M. and Yasmin, N. One-dimensional dam break solutions for variable width channels. *J. Hydraul. Eng.*, 1997, **123,** 464–468.
15. Hirsch, C., *Numerical Computation of Internal and External Flows*, John Wiley and Sons, New York, 1992.
16. Jameson, A., Schmidt, W. and Turkel, E., Numerical solutions of the Euler equations by finite volume methods using Runga-Kutta time stepping schemes. In *AIAA 14th Fluid and Plasma Dynamics Conference*, Palo Alto, CA, AIAA, 1981, pp. 1259.
17. Jha, A. K., Akiyama, J. and Ura, M. Modeling unsteady open-channel flows—Modification to beam and warming scheme. *J. Hydraul. Eng.*, 1994, **120,** 461–476.
18. Katapodes, N. and Strelkoff, T. Computing two-dimensional dam break flood waves. *J. Hydraul. Div., ASCE*, 1988, **110,** 1269–1288.
19. Meissner, U. A finite difference element integration scheme for long period water wave propagation. *Int. J. Num. Methods Eng.*, 1978, **12,** 1161–1169.
20. Rahman, M. and Chaudhry, M. H. Simulation of hydraulic jump with grid adaptation. *J. Hydraul. Res.*, 1995, **33,** 555–569.
21. Rahman, M. and Chaudhry, M. H. Simulation of dam-break with grid adaptation. *Advances in Water Resources*, 1998, **21,** 1–9.
22. Shu, C. W. and Osher, S. Efficient implementation of essentially non-oscillatory shock capturing schemes. *J. Comput. Phys.*, 1988, **77,** 439–471.
23. Vanleer, B. Towards the ultimate conservative difference scheme, II, monoticity and second order combined in a second order scheme. *J. Comput. Phys.*, 1973, **14,** 357–393.
24. Whitham, G. B., *Linear and Non Linear Waves*. John Wiley, New York, 1974.
25. Zalesak, S. T. Fully multidimensional flux-corrected transport algorithms for fluids. *J. Comput. Phys.*, 1979, **31,** 335–362.